

논문 17-11-12

## SAXS와 AFM에 의한 HF-용액내 양극 에칭에 의해 제조된 기공성 실리콘의 구조연구

### SAXS and AFM Study on Porous Silicon Prepared by Anodic Etching in HF-based Solution

김유진<sup>1,a</sup>, 김화중<sup>1,2</sup>  
(Eugene Kim<sup>1,a</sup> and Hwa Joong Kim<sup>1,2</sup>)

#### Abstract

Porous silicon materials have been shown to have bright prospects for applications in light emitting, solar cell, as well as light- and chemical sensing devices. In this report, structures of porous silicon prepared by anodic etching in HF-based solution with various etching times were studied in detail by Atomic Force Microscopy and Small Angle X-ray Scattering technique using the high energy beam line at Pohang Light Source in Korea. The results showed the coexistence of the various pores with nanometer and submicrometer scales. For nanometer size pores, the mixed ones with two different shapes were identified: the larger ones in cylindrical shape and the smaller ones in spherical shape. Volume fractions of the cylindrical and the spherical pores were about equal and remained unchanged at all etching times investigated. On the whole uniform values of the specific surface area and of the size parameters of the pores were observed except for the larger specific surface area for the sample with the short etching time. The results implies that etching process causes the inner surfaces to become smoother while new pores are being generated. In all SAXS data at large Q vectors, Porod slope of -4 was observed, which supports the fact that the pores have smooth surfaces.

**Key Words** : Porous silicon, Small angle x-ray scattering, Atomic force microscopy

#### 1. INTRODUCTION

When silicon is under anodic bias, porous silicon (PS) formation was observed as long as the reaction is limited by the charge supply of the electrode and not by ionic diffusion in the electrolyte. The discovery of the room-temperature photoluminescence of PS[1,2], with

the perspective of development of advanced silicon optoelectronic devices, has initiated the related researches extensively[3-5]. The properties of PS such as band gap broadening, absorption spectrum in the range of 0.8~1.3 eV, very good optical transmission by light with wave length of 700~1000 nm[6], and photoconductivity[7] have also attracted great interests. The details of formation and application of PS can be found in recent review paper[8].

PS obtained by anodic etching of mono-crystalline silicon in hydrofluoric(HF) acid solution showed strong luminescence in the visible range. Opto-electronic properties of this

1. 홍익대학교 분자전자공학대학원, 기초과학과  
(서울시 마포구 상수동 72-1)

2. (주)루벤텍스

a. Corresponding Author : kim@hongik.ac.kr

접수일자 : 2004. 7. 30

1차 심사 : 2004. 9. 13

심사완료 : 2004. 9. 21

material depend highly on specific surface area, structure of the pores and doping level of the silicon substrate. Various models have been invoked to try to explain the rich variety of porous Si structures[7,9]. The presence of large and small voids has been analyzed[10], but the detailed structures of pores in PS materials has not yet been completely elucidated.

In this study, Small Angle X-ray Scattering (SAXS) and Atomic Force Microscopy (AFM) were used to investigate the structural evolution of p-type doped PS samples. Detailed quantitative investigations of morphology, size distribution, and roughness of the internal surface were made by SAXS measurements using the model calculations followed by fitting procedure. The roughness of the internal surface could also be analyzed by interpreting the scattering data.

The scattering theories used in this study are briefly summarized. The expression for the particle form factor  $P(Q)$  for spheres of radius  $R$  is as follows[11,12].

$$P_{sp}(Q) = \left| \frac{3j_1(QR)}{QR} \right|^2 = \left[ \frac{3\sin QR - QR\cos QR}{(QR)^3} \right]^2 \quad (1)$$

where  $j_1(x)$  is a spherical Bessel function of first order. That for cylinder having diameter  $a$  and height  $h$  is as follows.

$$P_{cy}(Q) = \int_0^{\pi/2} \frac{\sin^2(Qh \cos \beta)}{Q^2 h \cos^2 \beta} \cdot \frac{4J_1^2(Qa \sin \beta)}{Q^2 a^2 \sin^2 \beta} \sin \beta d\beta \quad (2)$$

where  $J_1$  is the cylindrical Bessel function of order 1. In the intermediate Q-range ( $1/h < Q < 1/a$ ), Eq. (2) can be approximated to

$$P_{cy}(Q) \approx \frac{\pi}{2Qh} \exp[(-Q^2 a^2/4)] \quad (3)$$

This form of expression is often used to obtain the radius of the cylinder. Plot of  $\ln[Q \cdot \frac{d\Sigma}{dQ}]$  vs.  $Q^2$  results in a straight line in the present situation, and the radius,  $a$ , could be

extracted from the slope.

Guiner has shown that at small values of  $QR_0$ , where  $R_0$  is the linear dimension of the particle[11],  $P(Q)$  is related to the radius of gyration  $R_g$ ,

$$R_g = \left[ \frac{\int_v r^2 \rho(r) dr}{\int_v \rho(r) dr} \right]^{1/2} \quad (4)$$

It was shown that

$$P(Q) = \exp(-Q^2 R_g^2/3) \quad (5)$$

Equation 5 is valid typically for  $QR_g < 1$ . A plot of logarithm of scattered intensity versus  $Q^2$ , which is referred to as Guinier plot, thus allows the determination of  $R_g$  in the low Q region. The concept of  $R_g$  can be applicable to particles of any shape, but the effective Q-range where this parameter could be determined may vary with the shape.

For homogeneous particles with sharp boundaries with specific surface area,  $A_s$ , it can be shown at large Q that

$$\frac{d\Sigma}{dQ} = n(\rho_p - \rho_m)^2 \frac{2\pi A_s}{Q^4} \quad (6)$$

This is referred to as Porod Law[12], and is applicable typically when  $QR_0 \gg 5$ , which could be used to find the mean surface area of the particle.

## 2. EXPERIMENTALS

Porous silicon films were prepared by anodic etching of Boron doped p-type Si (100) wafers in aqueous HF solution mixed with ethanol in a volumetric ratio of 1:1 at various etching times at the 20 mA/cm<sup>2</sup> anodization current density (Table 1). The other side of the films was coated with alumina.

**Table 1.** Investigated p-type porous silicon samples.

Sample No.	Thickness (μm)	Etching Time (min)
0	50	0
1	50	100
2	75	150
3	100	300

The SAXS measurements[13,14] were performed in transmission geometry at Pohang Accelerator Lab. in Korea (Fig. 1). A 1-D Si diode-array detector was used with scattering vector ( $Q$ ) ranging from 0.005 to 0.25 Å<sup>-1</sup> with  $Q = 4\pi \sin \frac{\theta}{\lambda}$ , where  $2\theta$  is the scattering angle and  $\lambda = 1.504$  Å is the X-ray wavelength used. The distance from the sample holder to the detector was 1120 mm, from which  $\theta$  could be determined. Photon flux was approximately 1010 photons/sec and energy resolution ( $\Delta E/E$ ) was  $5 \times 10^{-4}$ . The beam size at the focal point was typically less than 1 mm<sup>2</sup>.

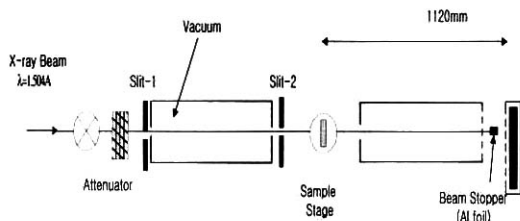


**Fig. 1.** SAXS instrument geometry.

### 3. RESULTS AND DISCUSSIONS

Figure 2 shows the AFM image of the not etched silicon wafer and the ones which was etched for various times. After etching, the formation of smoother surface undulation with sub-μm size is seen.

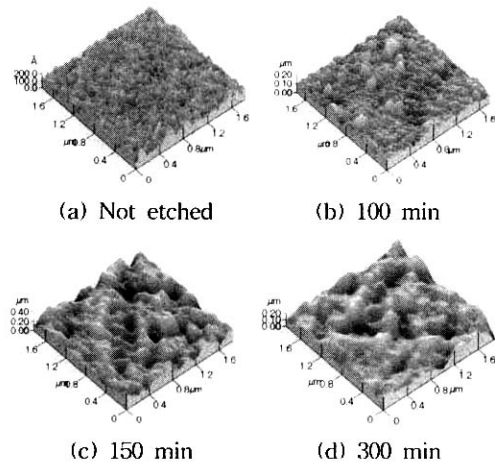


**Fig. 2.** AFM images of PS surfaces at different etching times.

The sample data reduction equation adopted was

$$I_{cor} = (I_{sam} - I_{bgd}) - [T_{sam}/T_{emp}](I_{emp} - I_{bgd}) \quad (7)$$

where  $I$ ,  $T$ ,  $_{sam}$ ,  $_{emp}$ , and  $_{bgd}$  represent the scattered intensity, transmission, sample, empty cell, and background, respectively. Figure 3 shows the SAXS data calibrated for dark current, background and detector efficiency. In order to obtain quantitative information on the pore size distribution, model calculations assuming the given size distributions were carried out to fit the data over the complete  $Q$ -range. Multiple scattering could be neglected for interpreting these data.

The overall structure of porous Si layer depends strongly upon anodization condition and the resistivity of the Si itself. Pore diameters and spacing can vary over a wide range from the nanometer scale up to the micron scale. The analysis of SAXS data is made assuming an isotropic distribution at all  $Q$ , which becomes anisotropic at small  $Q$  if the X-ray beam is not perpendicular to the sample surface. This is what one expects if the scattering at small  $Q$  is caused by extended pores of cylindrical shape, oriented with their axis perpendicular to the surface.

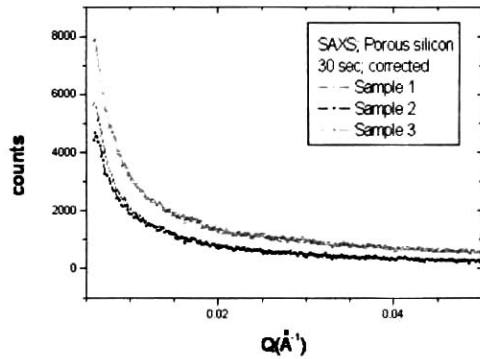


Fig. 3. SAXS data for three porous silicon samples collected for 30 sec using the beam with  $\lambda = 1.504 \text{ \AA}$ .

The morphology of silicon in the samples shows a bimodal distribution of pore shapes and sizes: small spherically shaped pores and large cylindrically shaped pores oriented with their axis perpendicular to the surface. This structural information could be obtained by the measurements that the sample was tilted with respect to the primary X-ray beam. In Fig. 4 the intensity on a log scale was plotted as a function of  $Q^2$ . In this so-called "Guinier plot" two straight lines are clearly present. From this it was judged that the morphology of the sample is composed of a bimodal size distribution in all cases. In the case of broad size distribution the Guinier method leads only to a rough estimate of the sizes. Model calculations with theoretical size distributions were therefore carried out to fit the data over the whole  $Q$ -range available. The best fits are shown in Fig. 5 together with the experimental data in which the intensity in absolute units is plotted as a function of  $Q$  on a double logarithmic scale. The fits obtained in this way using a bimodal size distribution are also shown in Fig. 4 using solid lines. The small pores have a well defined size with a maximum at  $1 \sim 15 \text{ \AA}$  and the average diameter of the cylindrically shaped pore was  $145 \sim 159 \text{ \AA}$  with a full width at half maximum of approximately

$60 \text{ \AA}$ . Figure 6 shows the bimodal size distribution of two kinds of pores used for the fitting of the data. The volume fractions of the large and the small pores were approximately the same. The specific surface area could also be calculated from the data at large  $Q$ . With increasing porosity with time, decrease in the size of the spherical pores were found, whereas the diameter of the large cylindrical pores remained approximately same. Specific surface area for sample 2 and 3 were nearly identical, while sample 1 showed a larger value. The results obtained from the SAXS measurements are compiled in Table 2.

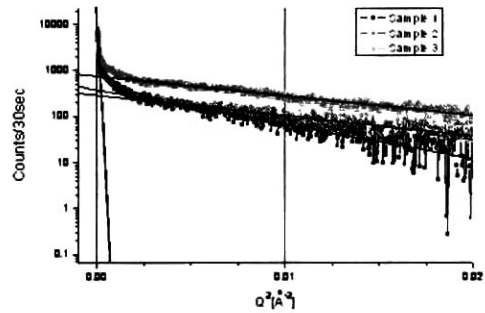


Fig. 4. Log I vs  $Q^2$  plot.

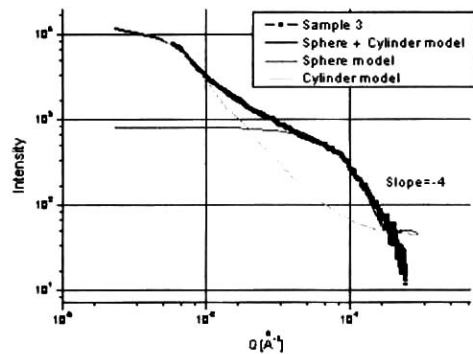


Fig. 5. SAXS intensity of p-type doped PS as a function of scattering vector ( $\log(d\Sigma/dQ)$  vs.  $\log Q$  plot) together with the model calculation for small pores, large pores, and the sum of both.

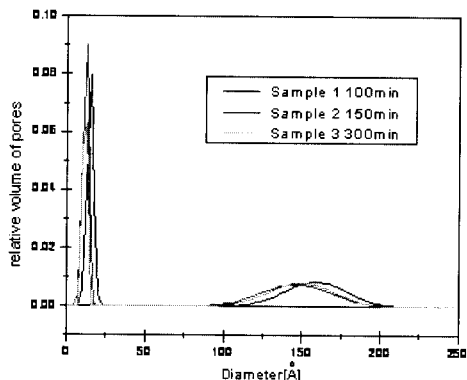


Fig. 6. Bimodal size distribution of spherical and cylindrical pores.

Table 2. The size parameters of the pores and specific surface area.

Sample no.	1	2	3
Average size of the spherically shaped pores(Å)	15	12	11
Average diameter of the cylindrically shaped pores(Å)	159	147	145
Specific Surface Area	208	160	161

For large Q values, the intensity in Fig 5 followed a Porod slope of -4 (Table 3) which indicates that the small spherical pores had a smooth surface. Interpretation of the scattering data at large Q range led us to conclude that there is no evidence that the rough internal surface which is likely to accompany with the fractal structures in porous silicon is present.

Table 3. The value of exponent n in porod plot.

Sample No.	n
1	4.2
2	4.0
3	3.8

#### 4. CONCLUSIONS

SAXS and AFM were used for the investigation of the structures of p-type doped PS materials etched in different extents. Various model calculations were adopted for interpreting SAXS data. The morphology and size distribution of the pores formed at different reaction times in PS films could be determined. A bimodal size distribution could adequately fit the intensity distribution. The volume fractions of the large cylindrical pores and the small spherical pores were approximately same. Almost uniform values of the specific surface area and of the size of the cylindrical pore diameters were observed except for the fact that the specific surface area for the shortest etching time was larger. Porod slope of -4 was observed at large Q, which indicates that our model calculation shows that considering fractal structures in explaining the pore development process is not necessary.

#### REFERENCES

- [1] L. T. Canham, "Silicon quantum wire array fabrication by electrochemical and chemical dissolution of wafers", Appl. Phys. Lett., Vol. 57, p. 1046, 1990.
- [2] S. S. Iyer, R. T. Collins, and L. T. Canham, "Light emission from silicon", Mater. Res. Soc. Symp. Proc., Vol. 256, 1992.
- [3] Seong Jeon Kim, Sang Hoon Lee, Bok Gil Choi, and Man Young Sung, "C-V response properties of alcohol vapor sensors based on porous silicon", J. of Kieeme(in Korean), Vol. 17, No. 6, p. 592, 2004.
- [4] Joo won Lee, Hoon Kim, Yun Hi Lee, Jin Jang, and Byeong Kwon Ju, "Electron emission from porous Poly-silicon nano-device for flat panel isplay", J. of Kieeme(in Korean), Vol. 16, p. 330, 2003.
- [5] Seong Jeon Kim, Sang Hoon Lee, and Bok Gil Choi, "Sensing properties of porous silicon layer for organic vapors", J. of Kieeme(in Korean), Vol. 15, No. 11, p. 963, 2002.

- [6] N. Koshida and H. Koyama, "Visible electro and photoluminescence from porous silicon and its related optoelectronic properties", Proc. Mat. Res. Soc. Symp., Vol. 256, p. 219, 1992.
- [7] V. Lehman and U. Gosele, "Porous silicon formation: A quantum wire effect", Appl. Phys. Lett., Vol. 58, p. 856, 1991.
- [8] H. Föll, M. Christophersen, J. Carstensen, and G. Hasse, "Formation and application of porous silicon", Materials Science and Engineering R, Vol. 39, p. 93, 2002.
- [9] D. Bellet, and G. Dolino, "X-ray diffraction studies of porous silicon", Thin Solid Films, Vol. 276, p. 1, 1996.
- [10] V. Vezin, P. Goudeau, and A. Naudon, "Characterization of photoluminescent porous Si by small angle scattering of X-rays", Appl. Phys. Lett., Vol. 60, p. 2625, 1992.
- [11] O. Glatter and O. Kratky, "Small-angle X-ray Scattering", Academic Press, London, p. 17, 1982.
- [12] S. Shih, K. H. Jung, T. Y. Hsieh, J. Sarathy, J. C. Campbell, and D. L. Kwong, "Photoluminescence and formation mechanism of chemically etched silicon", Appl. Phys. Lett., Vol. 60, p. 1863, 1992.
- [13] H. Franz, V. Petrova-Koch, T. Muschnik, and J. Peisl, "SAXS measurements", Mat. Res. Soc. Symp. Proc., Vol. 283, p. 133, 1993.
- [14] A. Guinier, "X-ray Diffraction", Freeman, London, 1963.